



CHORUS

This is the accepted manuscript made available via CHORUS. The article has been published as:

Reynolds-number power-law scaling of differential molecular diffusion in turbulent nonpremixed combustion

Chao Han and Haifeng Wang

Phys. Rev. Fluids **3**, 103201 — Published 10 October 2018

DOI: [10.1103/PhysRevFluids.3.103201](https://doi.org/10.1103/PhysRevFluids.3.103201)

Reynolds-number power-law scaling of differential molecular diffusion in turbulent non-premixed combustion

Chao Han and Haifeng Wang*

School of Aeronautics and Astronautics, Purdue University, West Lafayette, Indiana 47907, USA

(Dated: September 21, 2018)

A full understanding of differential molecular diffusion (DMD) in turbulent combustion has its theoretical significance for improving models of turbulent combustion. The scaling of the effect of DMD with respect to the Reynolds number in turbulent combustion is of particular interest for developing physically consistent modeling approaches for DMD. Such a scaling has been so far mostly studied in simple non-reacting flow problems, and a simple power-law scaling has been reported before. The applicability of the power-law scaling to turbulent combustion problems where the chemical reaction is expected to strongly couple with DMD has not been thoroughly studied. In this work, we aim to examine such a scaling by developing a statistical analysis of the dependence of DMD on the Reynolds number in turbulent non-premixed combustion. Three Sandia temporally evolving planar jet non-premixed CO/H₂ DNS flames (E.R. Hawkes, R. Sankaran, J.C. Sutherland, and J.H. Chen, *Proceedings of the Combustion Institute*, 31(1): 1633-1640, 2007) are chosen as the target flames for the study. The Reynolds-number-scaling based on a statistical analysis is reported, which is found to be statistically consistent with previous theoretical results in non-reacting problems. The results provide supportive evidence to the existence of a universal power-law scaling of the effect of DMD with respect to the Reynolds number in turbulent non-reacting and reacting flow problems. The results are also important for constraining the development of Reynolds-number-scaling consistent physical models for treating DMD in the modeling and simulations of multicomponent turbulent diffusion systems.

* haifeng@purdue.edu

I. INTRODUCTION

Design improvement and optimization of combustion processes in combustion engines such as gasoline engines and gas turbines are needed regularly to meet more and more stringent design and regulatory requirements on emission. Computational and modeling tools of turbulent combustion have become vital for aiding the design and optimization of combustion processes. The success of computational and modeling tools highly relies on the accuracy of the models that are developed to describe the underlying physicochemical processes in combustion. It is an overarching issue to develop accurate and predictive models to improve the design of combustion configurations.

Turbulent combustion is a classic multi-scale, multi-physical, and highly nonlinear phenomenon, involving many physicochemical processes such as fluid dynamics, turbulence, molecular diffusion, chemical kinetics, radiation, multi-phase, heat transfer, and acoustics [1–3]. Among them, molecular diffusion in turbulent combustion is the main focus of this work. In a multi-component gas-phase system like combustion, a phenomenon called differential molecular diffusion (DMD) [4, 5] (or preferential molecular diffusion [6]) is encountered when the different components have different molecular diffusivities. The significance of DMD in turbulent combustion has been recognized for a while. In turbulent premixed flames, it has been demonstrated that DMD can strongly affect the turbulent flame speed [7], flame width [8], flame structures [9], flame instabilities [10], and local extinction [11]. In turbulent non-premixed flames, it has also been shown that DMD can significantly influence flame structures [12], local extinction [13], flame stabilization [14], and flame ignition [15, 16].

In the past modeling studies of turbulent combustion, the effect of DMD is often neglected, based on the assumption of negligible effect of molecular diffusion on scalar transport in high Reynolds number turbulent flows [1, 3]. The incorporation of DMD into turbulent combustion models has emerged only recently. Kronenburg and Bilger [17, 18] obtained equations including the DMD effect in the conditional moment closure (CMC) model and proposed an approach based on DNS to model the additional terms introduced by the incorporation of DMD. Reasonable results were demonstrated by incorporating DMD in CMC and more accurate NO formation rates were predicted in the near field of a turbulent jet flame. A similar work was reported in Ma and Devaud [19] where the CMC equations with the DMD effect for species and enthalpy were derived and the effect of non-unity Lewis numbers of species H and H₂ on the combustion fields was examined. In the transported probability density function (PDF) method [20], an approach to treat spatial DMD was presented by McDermott and Pope [21]. In this approach, the spatial molecular transport of scalars was modeled by a mean shift (MS) model in the composition space to replace the traditional random walk model in the physical space [22] which is unable to treat DMD. Zhang and Wang [23] improved the MS model by developing a variance-consistent mean shift (VCMS) model to yield consistent transport of scalar variance. In the flamelet models [24], a consistent laminar flamelet equation with DMD was derived by Pitsch and Peters [25] and can be incorporated into flamelet models straightforwardly. However, this model tends to significantly over-predict the effect of DMD, especially at the downstream locations of a turbulent jet flame [26]. Wang [5] argued that this over-prediction was due to the missing Reynolds-number-dependence of DMD in the model. A class of new DMD flamelet models, called linear differential diffusion (LDD) model and nonlinear differential diffusion (NDD) model, was developed by Wang [5] to incorporate the effect of Reynolds number on DMD in the flamelet models.

Developing accurate models for DMD relies on an accurate understanding of the statistics of DMD. A critically important aspect of DMD in turbulent flow problems is the scaling of the effect of DMD with respect to the Reynolds number, which is the focus of this work. To study this scaling, we need to establish a quantification method for DMD and an appropriate definition of the Reynolds number.

The effect of DMD is commonly quantified by a parameter $z_{\alpha\beta}$ [4, 5, 12, 27],

$$z_{\alpha\beta}(\mathbf{x}, t) = \xi_{\alpha}(\mathbf{x}, t) - \xi_{\beta}(\mathbf{x}, t), \quad (1)$$

$$\xi_{\alpha}(\mathbf{x}, t) = \frac{Y_{\alpha}(\mathbf{x}, t) - Y_{\alpha,ox}}{Y_{\alpha,fu} - Y_{\alpha,ox}}, \quad (2)$$

where \mathbf{x} is the physical space vector, t is time, Y_{α} is the mass fraction of element α , ξ_{α} is the mixture fraction defined based on the mass fractions of element α , Y_{α} , and the subscripts “*ox*” and “*fu*” denote the oxidizer boundary and the fuel boundary for a two-inlet non-premixed combustion system, respectively. The moments of $z_{\alpha\beta}$ and ξ_{α} in turbulent flames can be readily obtained by performing Favre averaging, *e.g.*, the mean $\tilde{z}_{\alpha\beta}(\mathbf{x}, t) = \tilde{\xi}_{\alpha}(\mathbf{x}, t) - \tilde{\xi}_{\beta}(\mathbf{x}, t)$ and the RMS $z_{\alpha\beta,RMS}(\mathbf{x}, t) = \left(\widetilde{z_{\alpha\beta}^2} - \tilde{z}_{\alpha\beta}^2 \right)^{0.5}$.

Different definitions of the Reynolds number can be used to study the DMD scaling. One definition is based on a bulk Reynold number,

$$Re_b = \frac{UL}{\nu}, \quad (3)$$

76 where U is a characteristic bulk velocity, L is a length scale and ν is the kinematic viscosity. This Re_b number is a
 77 characteristic Reynolds number representing a whole turbulence field. A local turbulent Reynolds number can also
 78 be defined based on the turbulence integral scales to study the DMD scaling,

$$79 \quad Re_t = \frac{ul}{\nu}, \quad (4)$$

80 where the integral turbulent velocity scale is defined as $u = \sqrt{2k/3}$, and the turbulent integral length scale is defined
 81 as $l = \sqrt{2k^3/3\varepsilon}$ [5]. Here k is the turbulent kinetic energy and ε is the turbulent kinetic energy dissipation rate. It
 82 is argued that the local turbulent Reynolds number is probably more appropriate for studying the DMD scaling since
 83 DMD is a small-scale local phenomenon.

84 Bilger and Dibble [4] suggested that $\tilde{z}_{\alpha\beta}$ and $z_{\alpha\beta,RMS}$ both follow a simple power-law scaling as Re_t^{-1} in turbulent
 85 flows. A different scaling of $z_{\alpha\beta,RMS} \sim Re_t^{-0.25}$, however, was reported in Kerstein *et al.* [28], Nilsen and Kosály
 86 [29], and Ulitsky *et al.* [30] for non-reacting flows. The extensibility of this power-law scaling of $z_{\alpha\beta,RMS} \sim Re_t^{-0.25}$
 87 found in non-reacting problems to reacting problems remains to be validated. Han *et al.* [27] attempted a scaling
 88 analysis of DMD in a series of Sandia CO/H₂ DNS flames and found that the power-law scaling of $z_{HC,RMS}$ ranges
 89 between $Re_b^{-0.04}$ to $Re_b^{-0.57}$, where Re_b is used for the scaling study. There are also reports in the literature that do
 90 not support evident power-law scaling of DMD in turbulent non-premixed flames (*e.g.*, Smith *et al.* [31] for H₂/CO
 91 flames). This work further examines the scaling of DMD in turbulent non-premixed flames with the goal to provide
 92 consistent results for the Reynolds-number-scaling.

93 The theoretical scaling, $\tilde{z}_{\alpha\beta} \sim Re_t^{-1}$ and $z_{\alpha\beta,RMS} \sim Re_t^{-0.25}$, can be readily explained. For the mean scalars,
 94 the molecular diffusion affects the scalar transport in turbulence only through the spatial molecular diffusion term
 95 which is inversely proportional to the Reynolds number. This leads to the scaling of DMD in terms of the mean $\tilde{z}_{\alpha\beta}$
 96 also inversely proportional to the Reynolds number. For the second-order moment, the molecular diffusion affects
 97 the transport in both the spatial molecular diffusion term and the dissipation term. The spatial molecular diffusion
 98 for the second-order moment is also inversely proportional to the Reynolds number, which also suggests the scaling
 99 of $z_{\alpha\beta,RMS} \sim Re_t^{-1}$. Meanwhile, Based on Kolmogorov's eddy cascading hypothesis and turbulent scalar spectrum
 100 [1, 28, 32], scalars dissipate at either the Batchelor scale [33] or the Oboukov-Corrsin scale [34] and the dissipation is
 101 found to be correlated to the reciprocal of the square root of the Reynolds number, and as a result the DMD effect
 102 through scalar dissipation is expected to have a Reynolds-number-scaling of $z_{\alpha\beta,RMS} \sim Re_t^{-0.25}$. Theoretically, the
 103 scaling of $z_{\alpha\beta,RMS} \sim Re_t^{-1}$ is anticipated in the situation where the spatial molecular transport effect dominates
 104 the dissipation effect, and the scaling of $z_{\alpha\beta,RMS} \sim Re_t^{-0.25}$ is evident when the dissipation is dominate. The latter
 105 case is general in real-life turbulence and hence the scaling $z_{\alpha\beta,RMS} \sim Re_t^{-0.25}$ is generally expected. The simple
 106 Reynolds-number-scaling of DMD has a solid physical basis for ideal turbulence. Its extensibility to real turbulence
 107 accompanied by chemical reaction remains to be confirmed. Once confirmed, the Reynolds-number-scaling of DMD
 108 will be useful for guiding the development of consistent DMD models as well as for validating the consistency of
 109 existing models. Wang [5] incorporated the Reynolds-number-dependence in the flamelet model for treating DMD
 110 and obtained excellent agreement of the flamelet predictions with the experimental measurements for the mean values
 111 $\tilde{z}_{\alpha\beta}$. The model consistency for the second-order moment of z , $z_{\alpha\beta,RMS}$, has not been examined and it is not clear
 112 what is the right Reynolds-number-scaling for the model to reproduce.

113 This work is motivated by the incomplete knowledge of the Reynolds-number-scaling of DMD in turbulent non-
 114 premixed flames. The objective of the work is to develop a statistical analysis to gain a consistent Reynolds-number-
 115 scaling of DMD in turbulent non-premixed flames by analyzing three Sandia CO/H₂ DNS flames [35]. The rest of
 116 the paper is organized as follows. Section II examines the three Sandia CO/H₂ DNS flames. Section III presents
 117 a statistical analysis to obtain the Reynolds-number-scaling of DMD in these flames. The conclusions are drawn in
 118 Section IV.

119 II. DIFFERENTIAL MOLECULAR DIFFUSION IN SANDIA CO/H₂ DNS FLAMES

120 Three Sandia DNS flames are chosen as the target flames for the Reynolds-number-scaling analysis of DMD. The
 121 DNS flame conditions, the characterization of DMD in the flames, and some sample statistics of the flames are briefly
 122 summarized in this section.

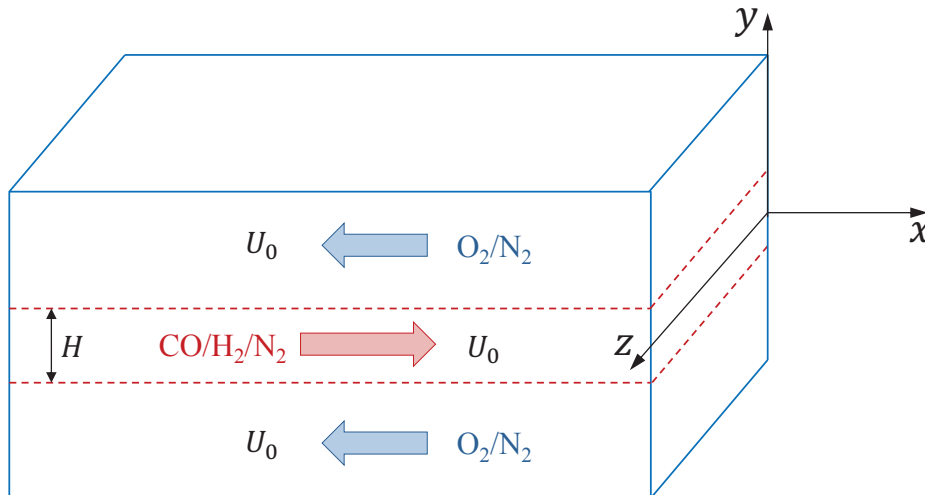


FIG. 1. The sketch of the Sandia temporally evolving jet CO/H₂ DNS flames [35].

TABLE I. The operating conditions of the Sandia CO/H₂ DNS flames [35].

	Case L	Case M	Case H
H [mm]	0.72	0.96	1.37
U_0 [m/s]	72.5	97	138
$Re_b = U_0 H / \nu$	2510	4478	9079
$t_0 = H / U_0$ [ms]	0.01	0.01	0.01
Da	0.011	0.011	0.011

A. Sandia CO/H₂ DNS flames

The flame configuration of the temporally evolving plane jet CO/H₂ DNS flames [35] is illustrated in Figure 1. The fuel stream consisting of 50% CO, 10% H₂, and 40% N₂ by volume flows at the center, and is surrounded by two counter-flowing oxidizer streams with 25% O₂ and 75% N₂ by volume. The stoichiometric mixture fraction is 0.42 based on the Bilger definition [36],

$$\xi_{Bilger} = \frac{\left(\frac{2Y_C}{M_C} + \frac{Y_H}{2M_H} - \frac{Y_O}{M_O}\right) - \left(\frac{2Y_{C,ox}}{M_C} + \frac{Y_{H,ox}}{2M_H} - \frac{Y_{O,ox}}{M_O}\right)}{\left(\frac{2Y_{C,fu}}{M_C} + \frac{Y_{H,fu}}{2M_H} - \frac{Y_{O,fu}}{M_O}\right) - \left(\frac{2Y_{C,ox}}{M_C} + \frac{Y_{H,ox}}{2M_H} - \frac{Y_{O,ox}}{M_O}\right)}, \quad (5)$$

where M_α is the molecular weight for the element α . Three flow conditions are available, Case L, Case M, and Case H, as summarized in Table I. In these flames, the initial fuel stream bulk velocity U_0 and the initial jet width H are adjusted to vary the bulk Reynolds number $Re_b = U_0 H / \nu$ while the flow time scale $t_0 = H / U_0$ is kept the same so that the Damkohler number $Da = \chi_{ex} t_0$ is the same ($\chi_{ex} = 2194 \text{ s}^{-1}$ is the extinction scalar dissipation rate limit in laminar opposed jet diffusion flames to represent the chemical time scale) [35]. The DNS domain size is $12H$ in the x -direction, $14H$ in the y -direction, and $8H$ in the z -direction. The grid resolution is uniform with the grid size $0.0208H = 0.015 \text{ mm}$, $0.0156H = 0.015 \text{ mm}$, and $0.0139H = 0.019 \text{ mm}$ for case L, case M, and case H, respectively. A periodic boundary condition is used in the x and z directions and a non-reflecting outflow boundary condition is used in the y direction. The compressible Navier-Stokes equations are solved with eighth-order explicit finite differencing in space, and fourth-order Runge-Kutta in time. For more details about the DNS cases, the readers are referred to the original DNS reference [35]. The fixed Da of the three cases provides a set of flames with the effect of the Reynolds number isolated so that the scaling of DMD with respect to the Reynolds number can be readily examined. The mixture-averaged diffusion model was used in the DNS to account for molecular diffusion. It has been shown that the mixture-averaged diffusion model is an adequate model for describing molecular diffusion in combustion [37] generally, and it is suitable for the current scaling study of the effect of DMD.

The turbulence characteristics of the DNS flames are shown in Figure 2 in terms of the spatial profiles of the turbulent kinetic energy k , the turbulent kinetic energy dissipation rate ε , the integral length scale l , the integral

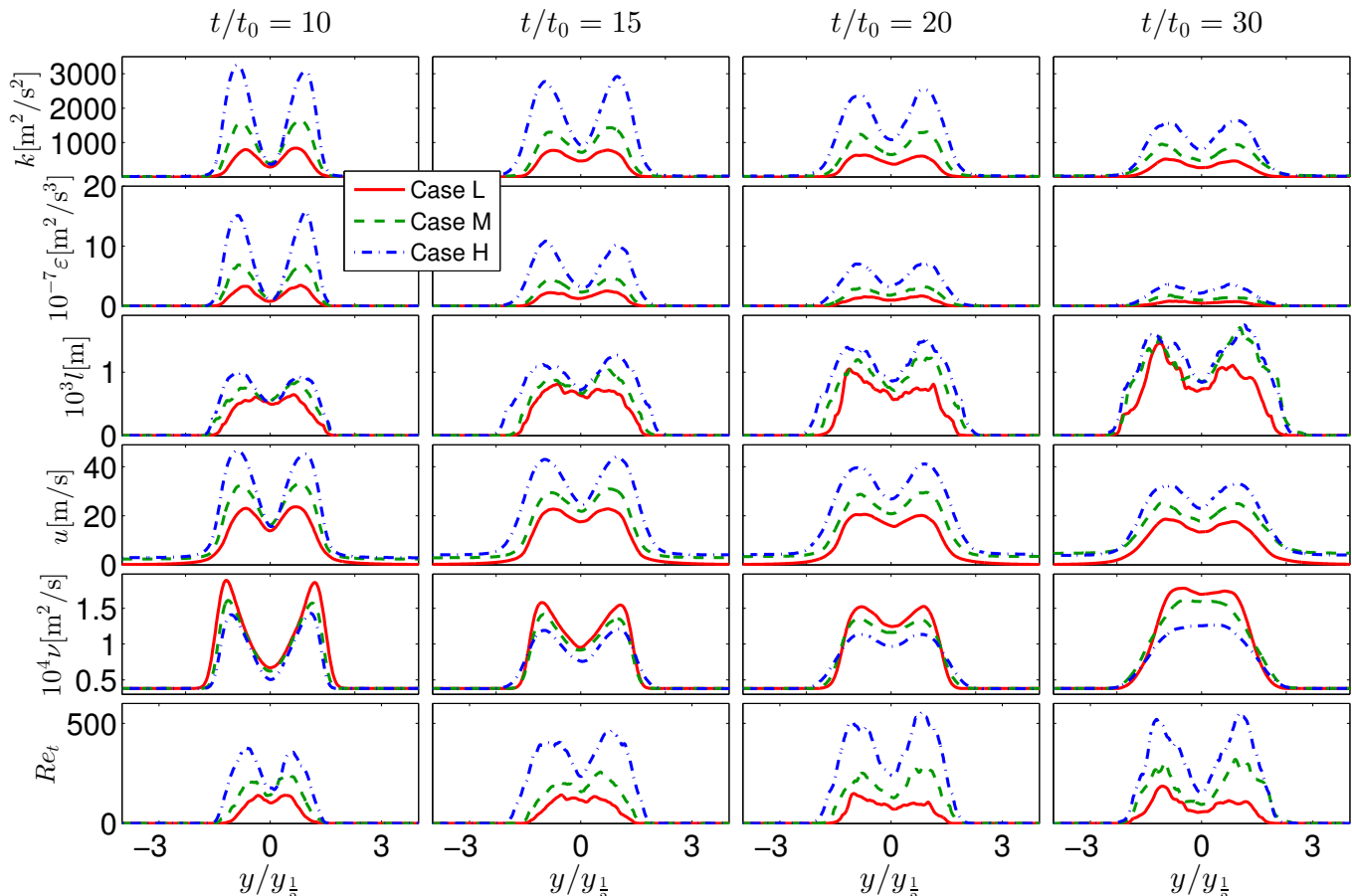


FIG. 2. The profiles of the turbulent kinetic energy k , the turbulence dissipation rate ε , the turbulence integral length scale l , the turbulence integral velocity scale u , the molecular viscosity ν , and the turbulent Reynolds number Re_t in the three Sandia CO/H₂ DNS flames [35] at the different times $t/t_0 = 10, 15, 20$ and 30 against y/y_{\perp} where y_{\perp} is the half width of the mixing layer based on the profiles of $\tilde{\xi}_C$.

146 velocity scale u , the kinematic viscosity ν , and the turbulent Reynolds number Re_t against y/y_{\perp} , where y_{\perp} is the half
 147 width of the mixing layer based on the profiles of $\tilde{\xi}_C$. The Favre-averaged statistics such as k and ε are obtained by
 148 averaging the DNS data in the span-wise direction z and the stream-wise direction x . All quantities that are shown
 149 in the figure exhibit double peaks around the two flame fronts. The increase of the bulk Reynolds number Re_b from
 150 case L to case H leads to the increase of k , ε , l , and u . The kinematic viscosity ν decreases with the increase of the
 151 Reynolds number mainly because of the decrease of flame temperature due to the increased flame local extinction
 152 from case L to case H. The local turbulent Reynolds number Re_t increases with the increase of Re_b .

153 B. Characterization of DMD in the Sandia CO/H₂ DNS flames

154 The effect of DMD is commonly quantified by $z_{\alpha\beta}$, $\tilde{z}_{\alpha\beta}$, and $z_{\alpha\beta,RMS}$. Different element pairs in equation (1),
 155 α and β , can be used to examine DMD in these DNS flames. Han *et al.* [27] demonstrated that the element pair,
 156 hydrogen H and carbon C, is representative to show the effect of DMD. In this work, we choose the elements H and
 157 C for examining the Reynolds-number-scaling of DMD, *i.e.*, in terms of \tilde{z}_{HC} and $z_{HC,RMS}$.

158 We first briefly examine the scalar statistics in the CO/H₂ DNS flames to provide an overview of the flames before
 159 we examine the scaling of DMD in Section III. Figure 3 shows the profiles of the mean mixture fraction $\tilde{\xi}_C$ (based
 160 on the element C), the RMS of mixture fraction $\xi_{C,RMS}$, the mean \tilde{z}_{HC} and the RMS $z_{HC,RMS}$ for the three CO/H₂
 161 DNS flames (Case L, Case M and Case H) at the different times $t/t_0 = 10, 15, 20$ and 30 against y/y_{\perp} . From the
 162 figure we can observe that the profiles of $\tilde{\xi}_C$ against y/y_{\perp} are only slightly different in the different flames at the same

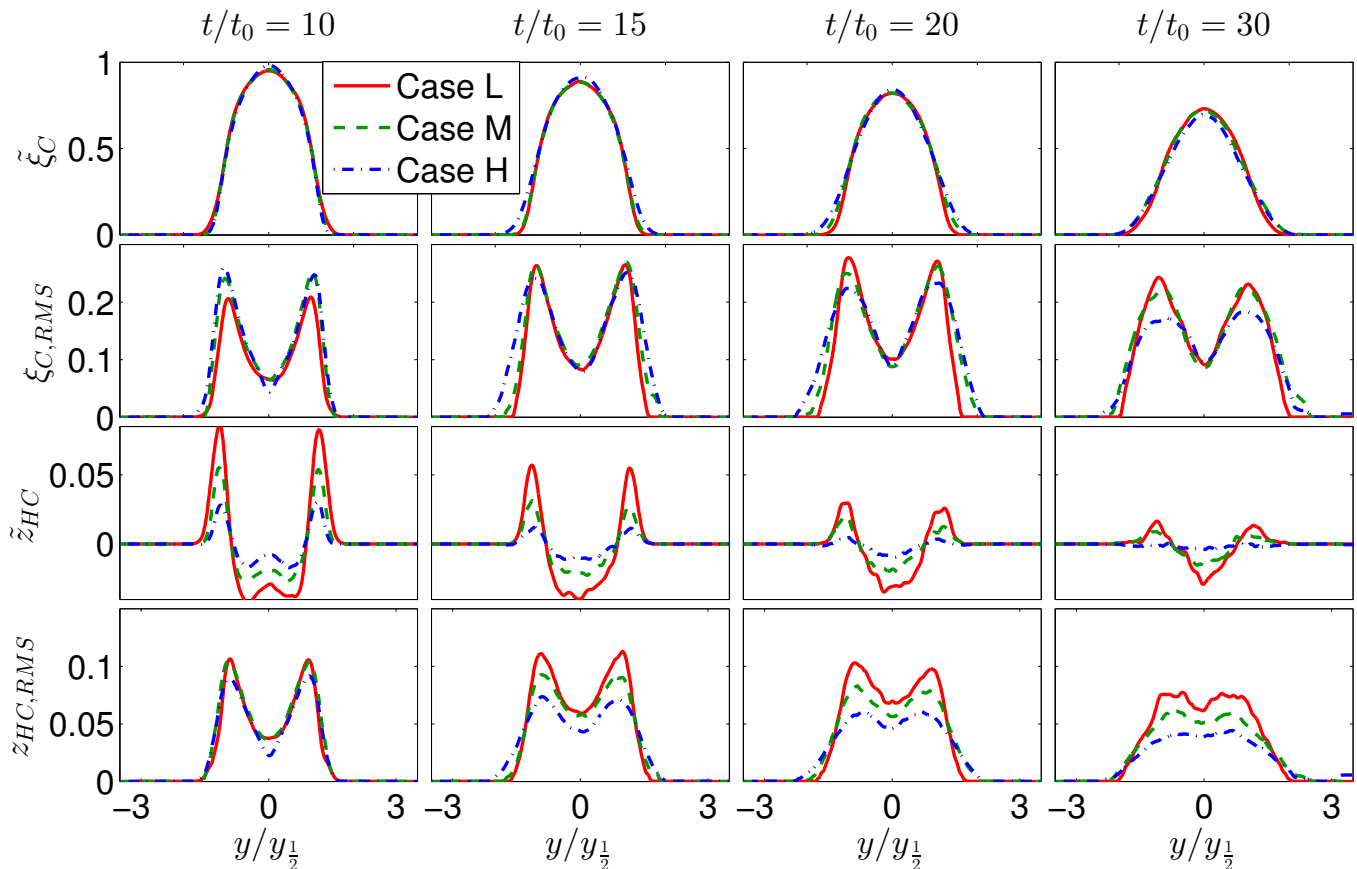


FIG. 3. the profiles of mean mixture fraction $\tilde{\xi}_C$, RMS of mixture fraction $\xi_{C,RMS}$, mean \tilde{z}_{HC} and RMS $z_{HC,RMS}$ against $y/y_{1/2}$ in the three Sandia CO/H₂ DNS flames at the different times $t/t_0 = 10, 15, 20$ and 30 .

163 t/t_0 , which indicates a weak sensitivity of $\tilde{\xi}_C$ to Re_b in the three cases. The profiles of $\xi_{C,RMS}$ against $y/y_{1/2}$ in Figure
 164 3 are influenced by Re_b slightly. At $t/t_0 = 10$, the peak value of $\xi_{C,RMS}$ increases with the increase of Re_b from Case
 165 L to Case H, while at $t/t_0 \geq 15$, the peak value decreases with the increase of Re_b . The peak magnitudes of \tilde{z}_{HC}
 166 and $z_{HC,RMS}$ are on the order of 0.1, and with the increase of Re_b from Case L to Case H, both \tilde{z}_{HC} and $z_{HC,RMS}$
 167 show the trend of decreasing, which is consistent with the theory that the effect of DMD decreases when the Reynolds
 168 number increases [4, 5]. The purpose of this paper is to find the quantitative Reynolds-number-scaling of the effect
 169 of DMD. From Figure 3, we can also see that the value of \tilde{z}_{HC} is negative on the fuel side while it is positive near
 170 the oxidizer side, which is caused by the higher molecular diffusion rate of light molecules such as H₂ and H.

171 In summary, an overview of the Sandia CO/H₂ DNS flames and some selected statistical results in the flames are
 172 provided in this section. The dependence of DMD on the Reynolds number is qualitatively examined. In the following
 173 Section III, we conduct analysis to gain quantitative Reynolds-number-scaling of such dependence.

174 III. SCALING ANALYSIS OF DIFFERENTIAL MOLECULAR DIFFUSION IN DNS FLAMES

175 A. Scaling Analysis Approach

176 We aim to gain a quantitative Reynolds-number-scaling of DMD from the three CO/H₂ DNS flames. Similar
 177 analyses have been reported before, mostly in non-reacting problems. A unique scaling of the mean $\tilde{z}_{HC} \sim Re_t^{-1}$ has
 178 been reported extensively (*e.g.*, Bilger and Dibble [4], Han *et al.* [27], Kerstein *et al.* [28], Bilger [38]). The scaling
 179 of the RMS $z_{HC,RMS}$ has also been studied but different scaling laws have been reported, *e.g.*, $z_{HC,RMS} \sim Re_t^{-1}$ [4]
 180 or $z_{HC,RMS} \sim Re_t^{-0.25}$ [28–30] based on theoretical studies. As discussed in Section I, both scalings for $z_{HC,RMS}$ can
 181 be explained theoretically but the latter one is likely the dominant scaling in real turbulence problems. The scaling
 182 of DMD has seldom been examined in real flames. Han *et al.* [27] attempted the analysis and obtained a power-law

183 scaling with the exponent varies widely in the Sandia CO/H₂ DNS flames, and hence produced inconsistent results
 184 with previous findings. It is not clear what is the cause of this inconsistency, and more work is needed to reconcile the
 185 different findings. This work serves as a significant extension of Han *et al.* [27] with the goal to obtain more consistent
 186 and reliable scaling results of DMD against the Reynolds number in turbulent non-premixed flames.

187 In Han *et al.* [27], the scaling of DMD was examined based on $\tilde{z}_{HC}(\mathbf{x}, t)$ and $z_{HC,RMS}(\mathbf{x}, t)$ against the bulk Reynolds
 188 number Re_b shown in Table 1. There are two problems with their analysis. First, in addition to the dependence on the
 189 Reynolds number, \tilde{z}_{HC} and $z_{HC,RMS}$ have other dependence such as on the local chemical compositions and scalar
 190 dissipation rate. The additional dependence, which was not considered in Han *et al.* [27], can potentially interfere
 191 with the Reynolds-number-scaling for z_{HC} and $z_{HC,RMS}$ and results in inconsistent results. Second, the Reynolds
 192 number used for the analysis in Han *et al.* [27] is the bulk Reynolds number Re_b as defined in Table I. DMD is a
 193 small-scale local phenomenon, and using a bulk Re_b is unlikely a suitable choice for revealing the true scaling that
 194 strongly depends on local turbulence level. This work chooses the same DNS flames and seeks a more rigorous analysis
 195 to isolate the dependence of DMD on the Reynolds number through conditioning in order to provide more reliable
 196 and consistent scaling results.

197 In general, in turbulent non-premixed flames, the statistics of z_{HC} such as \tilde{z}_{HC} and $z_{HC,RMS}$ depends on many
 198 parameters such as the statistics of the chemical compositions, Re_t , Da , and the Lewis number Le . In the Sandia
 199 CO/H₂ DNS flames, the fuel and oxidizer are fixed and hence Le is fixed among the three CO/H₂ DNS flames. The
 200 dimensionless number Da among the different flames is also fixed by design [35]. By employing the steady flamelet
 201 concept [24], *i.e.*, the chemical composition variables are approximately related to $(\tilde{\xi}_C, \xi_{C,RMS}, \tilde{\chi}_{st})$ where $\tilde{\chi}_{st}$ is the
 202 mean scalar dissipation rate at the stoichiometric condition, we can readily approximate \tilde{z}_{HC} and $z_{HC,RMS}$ as

$$203 \quad \tilde{z}_{HC} \approx \tilde{z}_{HC}(\tilde{\xi}_C, \xi_{C,RMS}, \tilde{\chi}_{st}, Re_t), \quad (6)$$

$$204 \quad z_{HC,RMS} \approx z_{HC,RMS}(\tilde{\xi}_C, \xi_{C,RMS}, \tilde{\chi}_{st}, Re_t), \quad (7)$$

205 where Re_t is added to the flamelet approximation to account for the dependence of DMD on it. In the following
 206 analysis, we examine the scaling of DMD by conditionally sampling the statistics $\tilde{z}_{HC}(\mathbf{x}, t)$ and $z_{HC,RMS}(\mathbf{x}, t)$ in the
 207 three Sandia CO/H₂ flames with the same values of $\tilde{\xi}_C$, $\xi_{C,RMS}$, and $\tilde{\chi}_{st}$, so that the sole dependence on Re_t can be
 208 better revealed.
 209

The DNS data used for this analysis contain the time history of the computed statistics (at about 250 sample time
 steps) by averaging in the span-wise direction z and the stream-wise direction x . The data are conditionally sampled
 into the following groups: $\tilde{z}_{HC}|_{\mathbf{C}}$ or $z_{HC,RMS}|_{\mathbf{C}}$ with the condition \mathbf{C} defined as,

$$\begin{aligned} \mathbf{C}(c_m, c_r, c_\chi) = & \left\{ \tilde{\xi}_C : \tilde{\xi}_C \in [c_m(1 - \epsilon_m), c_m(1 + \epsilon_m)] \right\} \\ & \cap \left\{ \xi_{C,RMS} : \xi_{C,RMS} \in [c_r(1 - \epsilon_r), c_r(1 + \epsilon_r)] \right\} \\ & \cap \left\{ \tilde{\chi}_{st} : \log_{10}(\tilde{\chi}_{st}) \in [c_\chi(1 - \epsilon_\chi), c_\chi(1 + \epsilon_\chi)] \right\}, \end{aligned} \quad (8)$$

210 where “ \cap ” denotes intersection, c_m and ϵ_m are used to define the conditioning interval for the mean $\tilde{\xi}_C$, c_r and ϵ_r
 211 for $\xi_{C,RMS}$, and c_χ and ϵ_χ for $\tilde{\chi}_{st}$. The finite sampling intervals are used in order to have enough data points under
 212 the condition. Ideally, the interval needs to be as small as possible to ensure accurate sampling under a particular
 213 condition, while it also needs to be big enough to have enough samples in the interval. In this work $\epsilon_m = 5 \times 10^{-3}$,
 214 $\epsilon_r = 8 \times 10^{-4}$, and $\epsilon_\chi = 0.2$ are used to balance these two considerations. Halving the values of these parameters
 215 yields a too small number of samples for the later probabilistic analysis. Doubling and tripling these parameters have
 216 been tried and they are found to have no significant effect on the results.

217 As argued in Section I, a local Reynolds number is needed to examine the DMD effect as a local phenomenon.
 218 Without using a local Reynolds number, Han *et al.* [27] reported a scaling factor for $z_{HC,RMS}$ ranged from $Re_b^{-0.04}$
 219 to $Re_b^{-0.57}$ when the bulk Reynolds number Re_b was used in the analysis. In this work, we use the local turbulent
 220 Reynolds number defined in equation (4).

221 By using the local Reynolds number, we can obtain a large number of data points with a range of Re_t corresponding
 222 to the three DNS flames, while with the bulk Re_b only three points from the three flames can be obtained [27] for the
 223 Reynolds-number-scaling analysis for DMD.

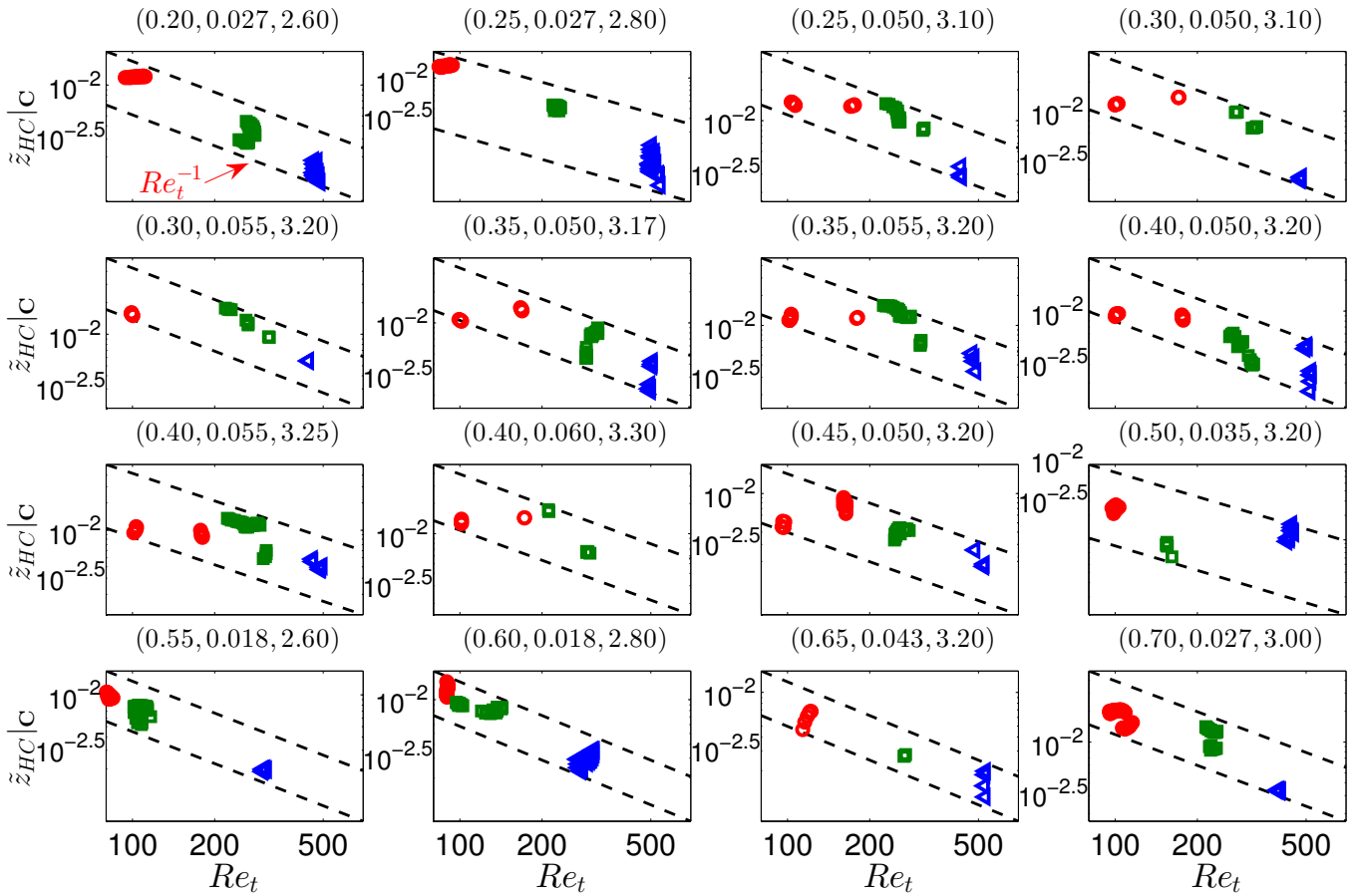


FIG. 4. The conditional average $\tilde{z}_{HC|C}$ against Re_t in the three CO/H₂ DNS flames. Red circles: Case L; Green squares: Case M; Blue triangles: Case H; dashed lines: reference lines with slope -1 in the log-log plot. The title of each sub-plot shows the condition $C(c_m, c_r, c_\chi)$ for computing the conditional average $\tilde{z}_{HC|C}$.

224

B. Scaling results for conditional statistics

225 The obtained results for $\tilde{z}_{HC|C}$ against Re_t are shown in Figure 4, for the various conditions C ($0.2 < c_m < 0.7$,
 226 $0.018 < c_r < 0.060$, $2.60 < c_\chi < 3.30$). The mean mixture fraction (c_m) in the range between $[0.2, 0.7]$ is chosen so that
 227 we can focus on the DMD effect near the flame front where the mixture fraction is close to the stoichiometric value of
 228 0.42. The mixture fraction RMS (c_r) is specified to be between $[0.018, 0.060]$ which covers most of the global limit of
 229 the mixture fraction RMS between $[0, 0.075]$ from all the three DNS flames. The scalar dissipation rate (c_χ) is chosen
 230 to be between $[10^{2.60} \text{ s}^{-1}, 10^{3.30} \text{ s}^{-1}]$ which also covers a significant portion of the global limit between $[0, 10^{3.65} \text{ s}^{-1}]$.
 231 The low dissipation rate range (say $c_\chi < 10^{2.6} \text{ s}^{-1}$) contains no sample data from the DNS flames when the ranges of
 232 the mixture fraction mean and RMS have been specified. The range of the conditional sampling variables is expected
 233 to cover most relevant regions in the DNS flames where DMD is of interest. From Figure 4, we can see that there is
 234 a clear trend of scaling Re_t^{-1} for the results of $\tilde{z}_{HC|C}$, by comparing the DNS results with the reference lines (dashed
 235 lines) with deviation of some results from the scaling. This, to some extent, provides a weak support to the scaling of
 236 Re_t^{-1} for \tilde{z}_{HC} obtained from the theoretical studies [4, 28, 38]. The exact scaling $\tilde{z}_{HC} \sim Re_t^{-1}$, however, is not seen
 237 in the Sandia DNS CO/H₂ flames.

238 The results for $z_{HC,RMS|C}$ against Re_t are shown in Figure 5 from the three DNS flames. Similarly, a trend of the
 239 power-law scaling of $Re_t^{-0.25}$ is seen from the results based on the comparison of the DNS results with the reference
 240 lines with slope -0.25 in the log-log plot, which supports the power-law scaling discussed in Kerstein *et al.* [28], Nilsen
 241 and Kosály [29], Ulitsky *et al.* [30] to some extent. Deviation of some results from the scaling is also apparent.

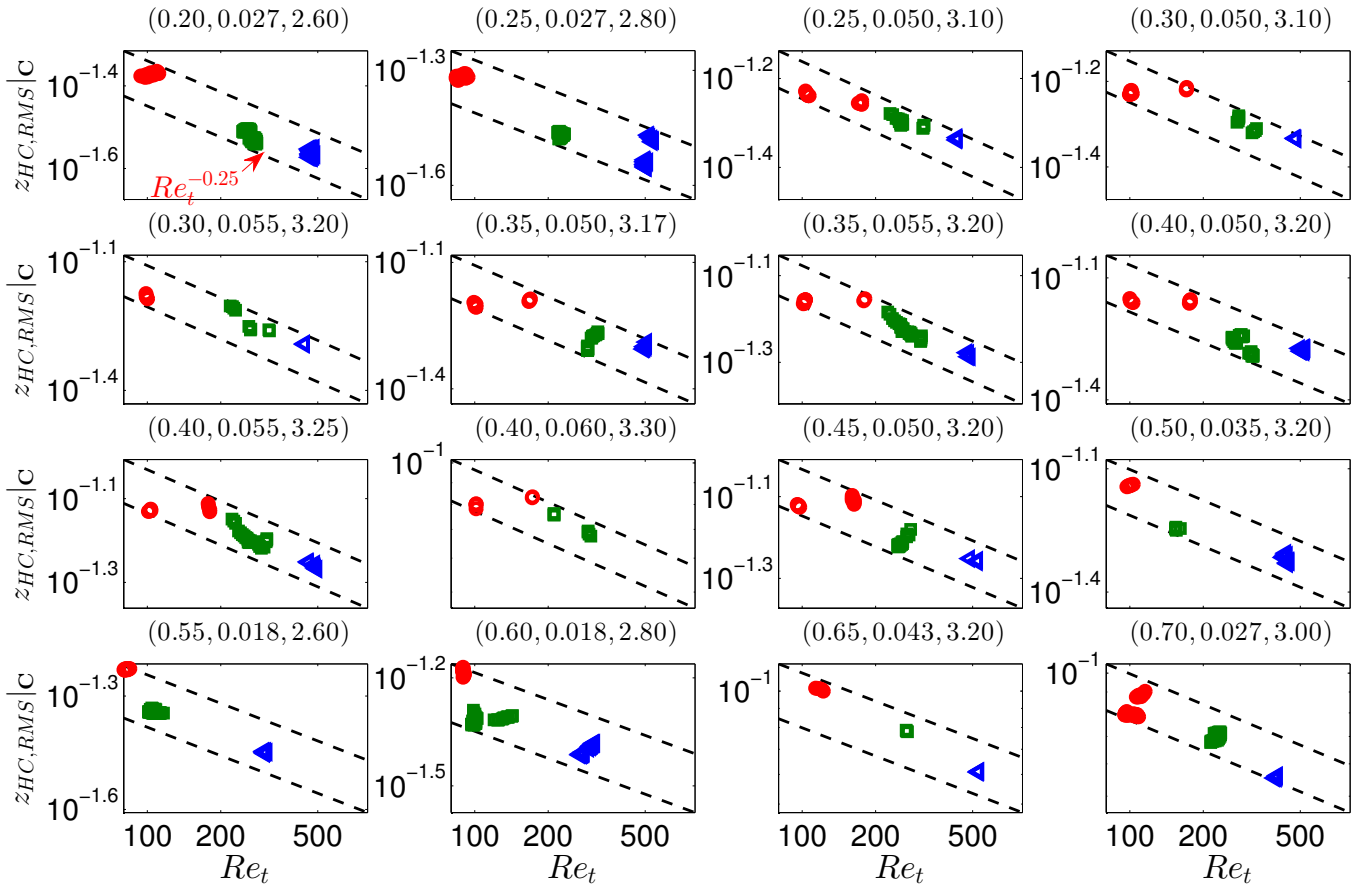


FIG. 5. The conditional ~~average~~ average of $z_{HC,RMS}|C$ against Re_t in the three CO/H₂ DNS flames. Red circles: Case L; Green squares: Case M; Blue triangles: Case H; dashed lines: reference lines with slope -0.25 in the log-log plot. **The title of each sub-plot shows the condition $C(c_m, c_r, c_x)$ for computing the conditional average $z_{HC,RMS}|C$.**

242

C. Probabilistic analysis of power-law scaling exponents

243 The results in Figures 4 and 5 provide some level of evidence to the power-law Reynolds-number-scaling in the
 244 Sandia CO/H₂ DNS flames that is consistent with the literature results [28–30] but also show some evident deviation.
 245 To understand these scaling results more thoroughly, we next employ a probabilistic analysis of the scaling law for
 246 \tilde{z}_{HC} and $z_{HC,RMS}$ in the Sandia DNS flames. We assume a scaling of $Re_t^{\kappa_m}$ for $\tilde{z}_{HC}|C$ and $Re_t^{\kappa_r}$ for $z_{HC,RMS}|C$,
 247 and write them as,

248

$$\ln \tilde{z}_{HC}|C \approx C_m + \kappa_m \ln Re_t, \quad (9)$$

249

250

$$\ln z_{HC,RMS}|C \approx C_r + \kappa_r \ln Re_t, \quad (10)$$

251 where C_m and C_r are parameters that are independent of Re_t , and κ_m and κ_r are the exponents for the power-law
 252 DMD scaling analysis. Based on the results in Figures 4 and 5, we cannot find universal constants for κ_m and κ_r
 253 in the DNS flames. Thus, instead of trying to seek constants (*e.g.*, $\kappa_m = -1$ and $\kappa_r = -0.25$) for a unique scaling of
 254 DMD, we view κ_m and κ_r as random variables. We aim to gain an understanding of the statistical distribution of
 255 κ_m and κ_r in the following analysis. The sample values of κ_m and κ_r can be obtained from the DNS results shown in
 256 Figures 4 and 5. From Figure 4, each pair of data points on the plots can be used to determine the values of C_m and
 257 κ_m by curving fitting using equation (9). We can use all different pairs of points in Figure 4 to collect the statistical
 258 sample values of κ_m . The statistical samples of κ_r can be collected in the same way.

259 The probability density functions (PDF) of κ_m and κ_r , $f_{\kappa_m}(\psi_m)$ and $f_{\kappa_r}(\psi_r)$, where ψ_m and ψ_r are the sample
 260 space variables corresponding to the random variables κ_m and κ_r , respectively, can then be approximated from the
 261 statistical samples of κ_m and κ_r , respectively. The bootstrap re-sampling method [39, 40] is used to reduce the

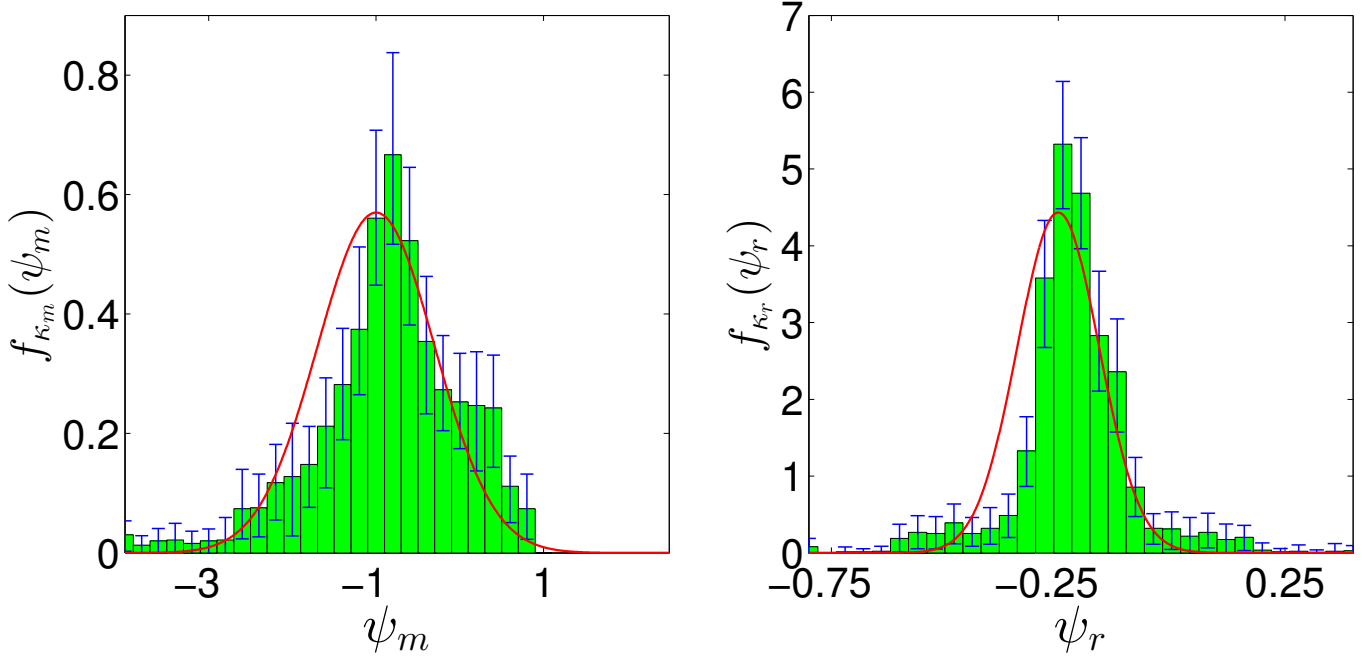


FIG. 6. The PDFs of scaling exponent κ_m (left) and κ_r (right). The solid lines are the ~~Classical~~ Gaussian PDF with the mean and variance ~~calculated~~ calculated from the data samples. The error bars are the estimated 95% confidence intervals.

262 statistical error in the computed PDFs. The basic idea of the bootstrap re-sampling is to generate new sets of samples
 263 of κ_m and κ_r from the original dataset for the estimation of the PDFs. The resampling is done by randomly selecting
 264 samples from the original dataset with replacement to form a new set with equal sample size. This resampling can be
 265 repeated multiple times. Each dataset (the original one or the new ones generated from re-sampling) can be used to
 266 compute the PDFs. The multiple PDFs computed from re-sampling can be averaged to form a PDF with a reduced
 267 statistical error. The standard deviation of the multiple PDFs can be calculated to estimate the 95% confidence
 268 interval to quantify the error in the estimation of the PDFs. Figure 6 shows the computed PDFs $f_{\kappa_m}(\psi_m)$ and
 269 $f_{\kappa_r}(\psi_r)$ with the estimated 95% confidence intervals. The bootstrap re-sampling is repeated 30 times for generating
 270 the PDFs in the figures. Both $f_{\kappa_m}(\psi_m)$ and $f_{\kappa_r}(\psi_r)$ show a ~~Classical~~ Gaussian-like probability distribution.
 271 The PDF $f_{\kappa_m}(\psi_m)$ peaks at $\psi_m \approx -1$, and $f_{\kappa_r}(\psi_r)$ peaks at $\psi_r \approx -0.25$. This provides, in a statistical sense,
 272 a strong support to the DMD scaling $\tilde{z}_{HC} \sim Re_t^{-1}$ and $z_{HC,RMS} \sim Re_t^{-0.25}$. These scaling can only be observed
 273 statistically, *i.e.*, the probability of finding these scaling exponents is the highest when compared with other values.
 274 The statistical results of $\tilde{z}_{HC} \sim Re_t^{-1}$ are consistent with the theoretical results from the literature. The finding of
 275 $z_{HC,RMS} \sim Re_t^{-0.25}$ supports those in Kerstein *et al.* [28], Nilsen and Kosály [29], and Ulitsky *et al.* [30]. The other
 276 scaling result $z_{HC,RMS} \sim Re_t^{-1}$ [4] is not supported by the current findings, which confirms the speculation discussed
 277 in Section I (the scaling $z_{HC,RMS} \sim Re_t^{-0.25}$ dominates the Re_t^{-1} scaling in real turbulence).

278 The exact scaling, $z_{HC} \sim Re_t^{-1}$ and $z_{HC,RMS} \sim Re_t^{-0.25}$, has a sound theoretical basis in idealized turbulence as
 279 discussed in Section I. The deviation from the theoretical scaling observed in the Sandia DNS flames requires some
 280 further examination. First of all, the theoretical scaling is expected only at a sufficiently high Reynolds number where
 281 a wide inertial range exists. Deviation from the theoretical scaling can be seen from a simple analysis of a mixing layer
 282 problem by Wang [5] when the Reynolds number is low. **The examined DNS flames in this work covers only a small
 283 range of low to moderate Reynolds numbers. The relatively low Reynold number is expected to be the main cause
 284 of the scattering of the DMD-scaling exponents in Figure 6. Hypothetically, the variance of the scaling exponents in
 285 Figure 6 is inversely correlated with the Reynolds number. The higher the Reynolds number, the smaller the variance.
 286 Examining this hypothesis, however, requires DNS cases with a wider range of Reynolds numbers, and it can be done
 287 when new DNS flames with different Reynolds number become available in the future.** Secondly, the derivation of the
 288 theoretical scaling relies on an assumption of a turbulent energy spectrum, say the Kolmogorov -5/3 energy spectrum.
 289 It is important to recognize that this spectrum can only be observed in a statistical sense even when the Reynolds
 290 number is sufficiently high. Locally and instantaneously, statistical fluctuations can cause the energy spectrum to
 291 deviate from the theoretical -5/3 scaling and hence pollute the theoretical scaling of DMD. **This gives rise to a further
 292 scattering of the DMD scaling exponents in the currently examined DNS flames where the Reynolds numbers are not**

high enough. Thirdly, the chemical reaction in turbulent combustion problems likely interferes with turbulence and molecular diffusion to cause the deviation of the DMD scaling from the theoretical results. The existence of a flame front in turbulent combustion can significantly affect the molecular diffusion process. The increase of temperature near a flame front can substantially increase the value of the molecular diffusivity and hence affects the molecular diffusion. The flame front can also affect the molecular diffusion by increasing the scalar gradient significantly if the flame front is thin. Additionally, the density change caused by chemical reaction can deviate turbulence from theoretical turbulence with constant density even if the Reynolds number is high. All these factors can cause the statistical distribution of the scaling exponents in Figure 6. Last but not least, a number of assumptions are involved in the current probabilistic analysis of DMD in the Sandia DNS flames, including but not limited to the flamelet assumption in equations (8) and (9) and neglecting the variation of local Da . These assumptions can likely contaminate the theoretical scaling as well. It is noted that although the global Da number for all the three DNS flames is the same, the contribution of Da to the scattering of the scaling exponents in Figure 6 has likely been accounted for since the local Da number in all three DNS flames is not a constant. Similar to the choice of the Reynolds number for the DMD scaling analysis, the local Da number is a suitable choice for the examination of the dependence of the scaling exponents on the Da number. Such dependence is not considered in the current analysis and hence its neglect is another plausible cause of the scattering of the scaling exponents observed in Figure 6.

In summary, we conduct a thorough DMD scaling analysis in the Sandia CO/H₂ DNS flames. A plausible power-law Reynolds-number-scaling in turbulent non-premixed flames is reported for the first time. It is argued that it is more appropriate to interpret the DMD scaling with respect to the Reynolds number as a statistical result. These results support the theoretical findings obtained in simple and non-reacting flows. It can also explain why the DMD scaling is not evident in previous studies [27, 31], if the analysis was not done statistically with a sufficient number of samples. These results are expected to be significant for guiding future development and validation of physical models for DMD that can yield the desired power-law Reynolds-number-scaling [5]. In a separate work [41], we have attempted to investigate the turbulence modeling requirements to yields the observed power-law scaling of DMD.

IV. CONCLUSIONS

In this work, a scaling analysis of the effect of DMD with respect to the Reynolds number is performed in turbulent non-premixed flames. A DNS dataset of the Sandia CO/H₂ DNS flames is used to quantify the dependence of the effect of DMD on a local Reynolds number. A statistical analysis of this dependence shows that the effect of DMD on mean quantities has the highest probability of scaling Re_t^{-1} and the effect of DMD on RMS quantities has the highest probability of scaling $Re_t^{-0.25}$. A unique scaling, however, cannot be observed in the DNS flames. These statistical scaling results are consistent, in a statistical sense, with previous findings from the theoretical analysis in non-reacting problems, indicating insignificant effect of chemical reaction on the scaling of DMD with respect to Reynolds number. This finding is important to guide future model development and simulations to be consistent with physical scaling laws.

ACKNOWLEDGEMENTS

Acknowledgment is made to the Donors of the American Chemical Society Petroleum Research Fund (Grant Number 53781-DNI9) for support of this research. This paper is based upon work supported by the National Science Foundation under Grant no. CBET-1336075. This research was supported in part through computational resources provided by Information Technology at Purdue University, West Lafayette, Indiana.

-
- [1] S. B. Pope, *Turbulent flows* (Cambridge University Press, 2000).
 - [2] T. Poinso and D. Veynante, *Theoretical and numerical combustion* (RT Edwards, Inc., 2005).
 - [3] D. Veynante and L. Vervisch, "Turbulent combustion modeling," *Prog. Energy Combust. Sci.* **28**, 193–266 (2002).
 - [4] W. Bilger and R. W. Dibble, "Differential molecular diffusion effects in turbulent mixing," *Combust. Sci. Technol.* **28**, 161–172 (1982).
 - [5] H. Wang, "Consistent flamelet modeling of differential molecular diffusion for turbulent non-premixed flames," *Phys. Fluids* **28**, 035102 (2016).
 - [6] T. Takagi, Y. Yoshikawa, K. Yoshida, M. Komiyama, and S. Kinoshita, "Studies on strained non-premixed flames affected by flame curvature and preferential diffusion," *Proc. Combust. Inst.* **26**, 1103–1110 (1996).

- [7] D. C. Haworth and T. J. Poinso, “Numerical simulations of Lewis number effects in turbulent premixed flames,” *J. Fluid Mech.* **244**, 405–436 (1992).
- [8] D. H. Rowinski and S. B. Pope, “Computational study of lean premixed turbulent flames using RANS/PDF and LES/PDF methods,” *Combust. Theory Modelling* **17**, 610–656 (2013).
- [9] R. S. Barlow, M. J. Dunn, and G. Magnotti, “Preferential transport effects in premixed bluff-body stabilized CH_4/H_2 flames,” *Combust. Flame* **162**, 727–735 (2015).
- [10] P. Cambray and G. Joulin, “On moderately-forced premixed flames,” *Proc. Combust. Inst.* **24**, 61–67 (1992).
- [11] A. N. Lipatnikov and J. Chomiak, “Molecular transport effects on turbulent flame propagation and structure,” *Prog. Energy Combust. Sci.* **31**, 1–73 (2005).
- [12] R. S. Barlow, J. H. Frank, A. N. Karpetis, and J.-Y. Chen, “Piloted methane/air jet flames: transport effects and aspects of scalar structure,” *Combust. Flame* **143**, 433–449 (2005).
- [13] H. Wang and K. Kim, “Effect of molecular transport on PDF modeling of turbulent non-premixed flames,” *Proc. Combust. Inst.* **35**, 1137–1145 (2015).
- [14] W. Han, V. Raman, and Z. Chen, “LES/PDF modeling of autoignition in a lifted turbulent flame: analysis of flame sensitivity to differential diffusion and scalar mixing time-scale,” *Combust. Flame* **171**, 69–86 (2016).
- [15] V. Gopalakrishnan and J. Abraham, “Effects of multicomponent diffusion on predicted ignition characteristics of an n-heptane diffusion flame,” *Combust. Flame* **136**, 557–566 (2004).
- [16] D. Frederick and J. Y. Chen, “Effects of differential diffusion on predicted autoignition delay times inspired by H_2/N_2 jet flames in a vitiated coflow using the linear eddy model,” *Flow Turbul. Combust.* **93**, 283–304 (2014).
- [17] A. Kronenburg and R. W. Bilger, “Modelling differential diffusion in nonpremixed reacting turbulent flow: application to turbulent jet flames,” *Combust. Sci. Technol.* **166**, 175–194 (2001).
- [18] A. Kronenburg and R. W. Bilger, “Modelling differential diffusion in nonpremixed reacting turbulent flow: model development,” *Combust. Sci. Technol.* **166**, 195–227 (2001).
- [19] M. Ma and C. B. Devaud, “A conditional moment closure (CMC) formulation including differential diffusion applied to a non-premixed hydrogen-air flame,” *Combust. Flame* **162**, 144–158 (2015).
- [20] S. B. Pope, “PDF methods for turbulent reactive flows,” *Prog. Energy Combust. Sci.* **11**, 119–192 (1985).
- [21] R. McDermott and S. B. Pope, “A particle formulation for treating differential diffusion in filtered density function methods,” *J. Comput. Phys.* **226**, 947–993 (2007).
- [22] M. S. Anand and S. B. Pope, “Diffusion behind a line source in grid turbulence,” *Turbulent shear flows* **4**, 46 (1985).
- [23] P. Zhang and H. Wang, “Variance consistent mean shift particle model for treating differential molecular diffusion in transported PDF methods for turbulent reactive flows,” *Comput. & Fluids* **170**, 53–76 (2018).
- [24] N. Peters, “Laminar diffusion flamelet models in non-premixed turbulent combustion,” *Prog. Energy Combust. Sci.* **10**, 319–339 (1984).
- [25] H. Pitsch and N. Peters, “A consistent flamelet formulation for non-premixed combustion considering differential diffusion effects,” *Combust. Flame* **114**, 26–40 (1998).
- [26] H. Pitsch, E. Riesmeier, and N. Peters, “Unsteady flamelet modeling of soot formation in turbulent diffusion flames,” *Combust. Sci. Technol.* **158**, 389–406 (2000).
- [27] C. Han, D. O. Lignell, E. R. Hawkes, J. H. Chen, and H. Wang, “Examination of the effect of differential molecular diffusion in DNS of turbulent non-premixed flames,” *Int. J. Hydrogen Energy* **42**, 11879–11892 (2017).
- [28] A. R. Kerstein, M. A. Cremer, and P. A. McMurtry, “Scaling properties of differential molecular diffusion effects in turbulence,” *Phys. Fluids* **7**, 1999–2007 (1995).
- [29] V. Nilsen and G. Kosály, “Differentially diffusing scalars in turbulence,” *Phys. Fluids* **9**, 3386–3397 (1997).
- [30] M. Ulitsky, T. Vaithianathan, and L. R. Collins, “A spectral study of differential diffusion of passive scalars in isotropic turbulence,” *J. Fluid Mech.* **460**, 1–38 (2002).
- [31] L. L. Smith, R. W. Dibble, L. Talbot, R. S. Barlow, and C. D. Carter, “Laser Raman scattering measurements of differential molecular diffusion in turbulent nonpremixed jet flames of H_2/CO_2 fuel,” *Combust. Flame* **100**, 153–160 (1995).
- [32] L. Dialameh, M. J. Cleary, and A. Y. Klimenko, “A multiple mapping conditioning model for differential diffusion,” *Phys. Fluids* **26**, 025107 (2014).
- [33] G. K. Batchelor, “Small-scale variation of convected quantities like temperature in turbulent fluid part 1. general discussion and the case of small conductivity,” *J. Fluid Mech.* **5**, 113–133 (1959).
- [34] A. M. Obukhov, “Structure of the temperature field in a turbulent flow,” Army Biological Labs, Frederick, MD (1968).
- [35] E. R. Hawkes, R. Sankaran, J. C. Sutherland, and J. H. Chen, “Scalar mixing in direct numerical simulations of temporally evolving plane jet flames with skeletal CO/H_2 kinetics,” *Proc. Combust. Inst.* **31**, 1633–1640 (2007).
- [36] R. W. Bilger, S. H. Stårner, and R. J. Kee, “On reduced mechanisms for methane air combustion in non-premixed flames,” *Combust. Flame* **80**, 135–149 (1990).
- [37] C. Bruno, V. Sankaran, H. Kolla, and J. H. Chen, “Impact of multi-component diffusion in turbulent combustion using direct numerical simulations,” *Combust. Flame* **162**, 4313–4330 (2015).
- [38] R. W. Bilger, “Molecular transport effects in turbulent diffusion flames at moderate Reynolds number,” *AIAA J.* **20**, 962–970 (1982).
- [39] A. C. Davison and D. V. Hinkley, *Bootstrap methods and their application*, Vol. 1 (Cambridge university press, 1997).
- [40] P. Zhang, A. R. Masri, and H. Wang, “Studies of the flow and turbulence fields in a turbulent pulsed jet flame using LES/PDF,” *Combust. Theory Modelling* **21**, 897–924 (2017).
- [41] C. Han, T. Pant, U. Jain, and H. Wang, “Consistent modeling of differential molecular diffusion to yield desired Reynolds-number power-law scaling,” *Phys. of Fluids* **30**, 085108 (2018).